Legesse *Environ Syst Res (2016) 5:16*
DOI 10.1186/s40068-016-0066-1

Environmental Systems Research

RESEARCH

Open Access

# The outlook of Ethiopian long rain season from the global circulation model

Solomon Addisu Legesse*

## Abstract

**Background:** The primary reason to study summer monsoon (long rain season) all over Ethiopia was due to the atmospheric circulation displays a spectacular annual cycle of rainfall in which more than 80 % of the annual rain comes during the summer season comprised of the months June–September. Any minor change in rainfall intensity from the normal conditions imposes a severe challenge on the rural people since its main livelihood is agriculture which mostly relies on summer monsoon. This research work, entitled, 'The outlook of Ethiopian long rain season from the global circulation model' has been conducted to fill such knowledge gaps of the target population. The objectives of the research were to examine the global circulation model output data and its outlooks over Ethiopian summer. To attain this specific objective, global circulation model output data were used. These data were analyzed by using *Xcon*, *Matlab* and grid analysis and display system computer software programs.

**Results:** The results revealed that Ethiopian summer rainfall (long rain season) has been declined by 70.51 mm in the past four decades (1971–2010); while the best performed models having similar trends to the historical observed rainfall data analysis predicted that the future summer mean rainfall amount will decline by about 60.07 mm (model *cccma*) and 89.45 mm (model *bccr*).

**Conclusions:** To conclude, the legislative bodies and development planners should design strategies and plans by taking into account impacts of declining summer rainfall on rural livelihoods.

**Keywords:** Global circulation model, Climate change, Rainfall, Ethiopian summer, Long rain season

## Background

Ethiopia presents a particularly difficult test for climate models. The central part of Ethiopia is dominated by highland plateaus, which split the country into two climatically (Mikko et al. 2009). The south and east, the land is semi-arid and the rain falls in two short spells either side of the dry season of summer (June–August). The north and west, the vegetation is more bush, and summer is the major rainy season (Gulilat et al. 2008). This split in the geographical distribution of rainfall, and the different seasonal cycles in different regions of Ethiopia make the task of simulating Ethiopian rainfall extremely challenging. Furthermore, climate models need to be able to capture the processes that influence the year to year (inter-annual) variability of Ethiopian rainfall. Variations of El Nino, the Indian monsoon and the position of the African easterly jet, all influence the rainfall over Ethiopia (Gulilat et al. 2008).

Disentangling these remote influences on the climate characteristics of Ethiopia and properly simulating in a climate model is a remarkably difficult task (Gulilat et al. 2008). Seasonal rainfall in Ethiopia is driven mainly by the migration of the inter-tropical convergence zone (ITCZ). Most parts of Ethiopia have experienced one main wet season (called *Kiremt*) from mid-June to mid-September (up to 350 mm per month in the wettest regions), when the ITCZ is in its northern-most position (Gulilat et al. 2008). Parts of northern and central Ethiopia also have a secondary wet season of sporadic, and considerably lesser, rainfall from February to May (called *Belg*).

The southern regions of Ethiopia experience two distinct wet seasons which occur as the ITCZ passes through this more southern position (March–May) *Belg* season is the main rainfall season, yielding 100–200 mm monthly,

*Correspondence: soladd2000@yahoo.com
Department of Natural Resources Management, College of Agriculture and Environmental Sciences, Bahir Dar University, Bahir Dar, Ethiopia

© 2016 Legesse. This article is distributed under the terms of the Creative Commons Attribution 4.0 International License (http://creativecommons.org/licenses/by/4.0/), which permits unrestricted use, distribution, and reproduction in any medium, provided you give appropriate credit to the original author(s) and the source, provide a link to the Creative Commons license, and indicate if changes were made.

followed by a lesser rainfall season in October to December called *Bega* (around 100 mm per month) (world bank 2010). The eastern most corner of Ethiopia receives very little rainfall at any time of the year. The movements of the ITCZ are sensitive to variations in Indian Ocean sea-surface temperatures and vary from year to year, as the onset and duration of the rainfall seasons vary considerably inter-annually, causing frequent drought. According to Gulilat et al. (2008), the most well documented causes of this variability is the El Niño southern oscillation (ENSO). Warm phases of ENSO (El Niño) have been associated with reduced rainfall in the main wet season, July, August and September, in north and central Ethiopia, causing drought, but also with greater rainfalls in the early February to April rainfall season which mainly affects southern Ethiopia (Maugeri 2011). In addition to capturing the general patterns of rainfall, climate models should be able to provide a reasonable simulation of the seasonal cycle of rainfall. Because of the high spatial variation of rainfall over Ethiopia both in terms of the seasonal cycle and the inter-annual variability, Ethiopia is aggregated into a number of homogeneous rainfall zones (McSweeney et al. 2008).

The rural people of Ethiopia in general are dependent on summer rain for agricultural production activities (main livelihood of the country) (NMSA 2007). Hence, the specific objectives of this research was to examine the global circulation model output rainfall data over Ethiopian summer for the past 40 years (1971–2010) and its 40 years future predictions (2015–2054).

## Methods

Ethiopia is located in Northeastern or East Central Horn of Africa lying between 3 and 15 degrees north latitude, 33–48 degrees east longitude. Ethiopia is bordered in the east Somalia and Djibouti, in the south by Kenya, in the northeast by Eritrea and in the west by the North and South Sudan (newest country). The country has a total area of about 1.1 million km$^2$ and comprises of 12 river basins with varying size and water resource potential (CSA 2007). Ethiopia falls into four main geographic regions from west to east; the Great Rift Valley, the Somali plateau, the *Ogaden* plateau and the Ethiopian plateau. The Ethiopian plateau, fringed in the west by the Sudan lowlands (made up of savanna and forest), includes more than half of the country. It has several high mountains and is generally 1524–1829 m a.s.l high, but reaches a much loftier height including *Ras Dejen* (4620 m a.s.l), the highest point in Ethiopia. The plateau slopes gently from east to west and is cut by numerous deep valleys.

The materials and computer software programs which were used for this study are topographic map of Ethiopia, external hard disc, raw GCM output data and observed data, *Matlab, Xcon* and GrADS respectively.

For the accuracy and reliability of the real climate situation of the study area, observed climate station data from different sites and more sophisticated and recent models output data were used. GCMs output data were used to simulate the climatic effect of increased atmospheric concentration of greenhouse gases (GHGs) and the climate model output was interpolated to the scale of Ethiopia using a regular grid bilinear interpolation method. The interpolated climate data were consisting of inter-governmental panel on climate change (IPCC) core variable such as precipitation in the study area. This was determined by the local knowledge and experts' opinion of the study area. The performance of GCM was evaluated and the best model, which has a high hit rate for the observed data was used to predict the future summer monsoon (rainfall).

### GCM output data acquisition

For the period from 1971 to 2010 and from 2015 to 2054, appropriate scenarios were selected based on the data availability. These data represent a subset of the IPCC model output archive run by Program for Climate Model Diagnosis and Inter-comparison (PCMDI). The complete set of core data variables in monthly temporal resolution was obtained from the IPCC-data distribution center (IPCC-DDC 2007), at the website http://www.ipcc-data.org/gcm/monthly/SRES_AR4/index.html. Since the data were developed for global scale and is at a suitable spatial resolution, the extent of Ethiopia was considered for selected high performance model data output. This was done by bilinear interpolation *Xcon* computer program (Yatagai et al. 2009). In order to investigate climate change situations of Ethiopia, much higher spatial information was required. Our objectives in interpolating global scale climate data were twofold—firstly to be able to evaluate the spatial variability in more detail across Ethiopia and secondly to provide more specific climate variable data inputs for further research activities. The future climate predictions provide information on the actual values of climatic variables (e.g. precipitation, which are common in the study area).

### NCEP data

Observations are from many different sources, including satellites, ships, ground stations, and radar. Currently, earth system research laboratory, physical sciences division (PSD) makes available these reanalysis datasets to the public in standard *netCDF* file format at the website http://journals.ametsoc.org/doi/pdf/10.1175/15200477(1996)077%3C0437%3ATNYRP%3E2.0.CO%3B2.

Reanalysis is a method to reconstruct the past state of the atmosphere and oceans in a coherent way by combining available observations with numerical models. These reconstructions are created with model based data assimilation methods which are similar to those used for numerical weather prediction (Compo et al. 2011). NCEP reanalysis is also scientific method for developing a comprehensive record of how weather and climate are changing. Observations and a numerical model that simulates one or more aspects of the earth system are combined objectively to generate a synthesized estimate (Compo et al. 2011). A reanalysis typically extends over several decades or longer and covers the entire globe from the earth's surface to the top of the stratosphere. NCEP reanalysis products are used extensively in climate research and services classifying the causes of climate change and preparing climate predictions (IPCC 2007). A large subset of this data is available from PSD in its original four times daily format and as daily averages. Reanalysis datasets are created by assimilating ("inputting") climate observations using the same climate model throughout the entire reanalysis period in order to reduce the effects of modeling changes on climate statistics (Compo et al. 2011).

It is possible to extract useful information about rainfall, temperature and humidity observation from satellites, or to infer large-scale features of the global circulation in the early 20th century using only surface pressure observations available at that time (Compo et al. 2011). Reanalysis is a rapidly evolving field and new reanalysis products benefit from recent modeling capabilities, improved techniques in data assimilation, in the latest observation techniques (i.e. from satellite measurements), and newly digitalized historical datasets (Compo et al. 2011). Reanalysis also allows the user to estimate rainfall over regions where in situ observations are not available. This dataset for Ethiopian summer rainfall comprises monthly variables of each year from 1971 to 2010 at a resolution of 0.5 degrees (approximately 55 km at the equator) were downloaded and crucially contains the climate variables which are common parameters to Ethiopia. This period was selected since the observation data before 1971 was not reliable and digital in the case of Ethiopia. It has been since 1971 that modern and standardized meteorological weather instruments were installed by (World Meteorological Organization) WMO standards (NMSA 2007).

### Data analysis

According to Joel and Mike (2006) there are three generic types of climate change scenarios. These are scenarios based on outputs from GCMs, synthetic scenarios, and analogue scenarios. All the three types have been used in climate change impacts research; although probably a majority of impact studies have used scenarios based on GCMs output. For this research, scenario based on the outputs of GCM was used and the analysis procedures are stated in the following sections.

The historical summer monsoon (summer rainfall) was analyzed by dividing into two periods; 1971–1990 and 1991–2010 for the proper performance of the models as well as the past trends. This period was selected since the observation data before 1971 was not reliable and digital in the case of Ethiopia. This might serve also to avoid over generalization of the model values and for easy management and processing of the *netCDF* files. Studying the historical summer monsoon would also help to determine the trends of rainfall and to evaluate the best-performed model for forecasting the future (2015–2034 and 2035–2054) of summer rainfall conditions.

Data from a number of climate models run by different national meteorological organizations and for a wide range of climate variables under different SRES Scenarios are available. In accordance with current best practice for analyzing the outputs of climate modeling exercises, the data from six runs of six different climate models were used. The model name and its origin are given as: bccr-bcm2.0 (Norway), cccma_cgcm3_1 (Canada), giss_model (USA), inmcm3_0 (Russia), ipsl_cm4 (France), and mpi_echam5 (Germany) (Table 1).

A total of 23.6 GB data were downloaded and stored. The data were available in *netCDF* file format which is not a flat file construction, relatively a self-describing multi-layered structure for storing and documenting large amounts of numerical precipitation data files. Each file downloaded contains monthly precipitation data (i.e. a single value for each month of the year) for all years for the entire earth. In order to extract 'slices' of the multi-layered *netCDF* datasets, it was necessary to use certain tools which were designed specifically for the *netCDF* file format.

It was therefore freely downloadable computer software program which enabled to visualize and extract data

**Table 1 Summary of the models used for precipitation variable**

| No. | Country of run | Model name | Run | Precipitation |
|---|---|---|---|---|
| 1 | Norway | Bccr-bcm2.0 | 1 | √ |
| 2 | Canada | Cccma_cgcm3_1 | 1 | √ |
| 3 | USA | Giss_model_e_r | 1 | √ |
| 4 | Russia | Inmcm3_0 | 1 | √ |
| 5 | France | Ipsl_cm4 | 3 | √ |
| 6 | Germany | Echam-5 | 3 | √ |

slices from *netCDF*. Examples of these are the climate data analysis tools, which is a collection of applications based on the *Xcon* software. Using this software, both temporal (1971–2054) and spatial (from the global scale to Ethiopian latitudinal and longitudinal extent) slices of a *netCDF* file were extracted. It was important to recognize that from a temporal perspective, what was actually extracted were the monthly normal calculated from the data for 40 years either side of the year of interest. The reason for calculating monthly normal was to eliminate single year anomalies that may show up in data from a single year only. Due to the spatial sub-setting routine to remove data outside of Ethiopia, in addition to the calculation of monthly normal, the size of this entire data set was reduced from 23.6 GB to 210 MB. Further compression has reduced the total size of the dataset. The sample interpolation of the GCM output data is indicated by Fig. 1.

The mask file was prepared using excel sheet by putting a zero value for areas not touched and one value for areas

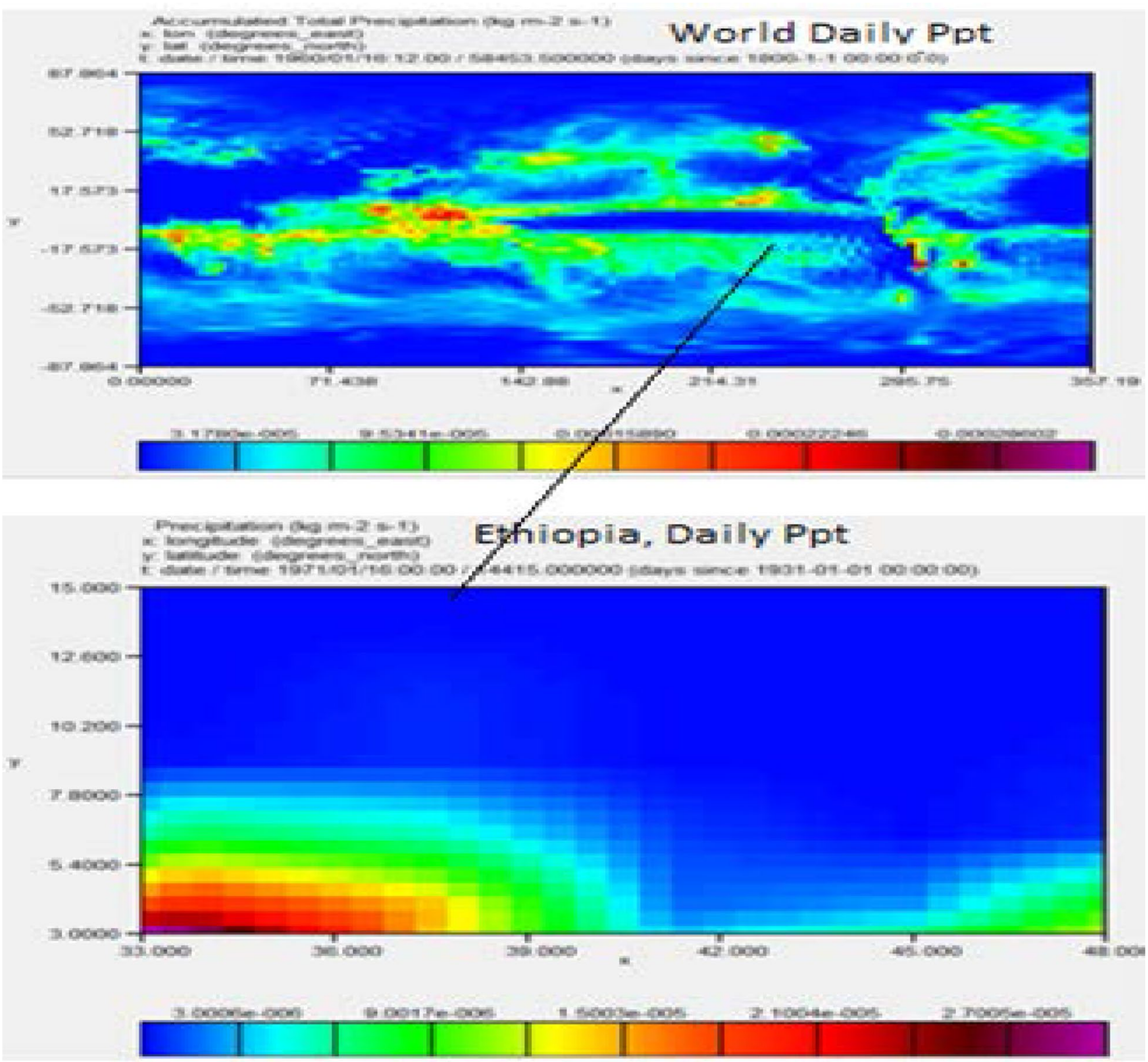


**Fig. 1** Interpolation rainfall into Ethiopia from *ipsl* model Source: computed by *Xcon* from *IPSL* model (2014)

covered by the latitudinal and longitudinal extent of Ethiopia. This value was used to limit the study only for the area covered by map of Ethiopia. The GCM output data were processed and studied for the whole parts of Ethiopia. This was done by downloading the GCM output data and interpolated to Ethiopian scale by 0.5 latitude and longitude. The mathematical modeling (*Matlab*) cod (program was developed to calculate the different statistical analysis, such as climatology (clim), standard deviation (SD), root mean square errors (rmse), coefficient of variations (cv) and correlations (corr).

## Results and discussions

### Summer monsoon from the GCM and the observed (1971–1990)

The time series year average (clim), the standard deviation (SD), the coefficient of variations (cv), the correlation (corr.), the root mean square errors (rmse) and the bias value of precipitation were used to evaluate the best performed model over Ethiopia. This would help to predict the future summer rainfall trends across the country. Accordingly, the models which have similar record of clim, sd and cv to that of the observed one would be taken as the best performed model. On the other hand, the smaller magnitude value of the rmse and bias would be selected as best performed and will be used to predict to the future summer rainfall amount provided that the trends should also be similar (Doswell et al. 2005). In other words, if the rmse computed value is greater or if the bias value between the model data and the observed data is greater, the performance of the model capturing that particular area climate situation is poor and unable to use such models for further predictions. This would happen due to the geographical location and the altitudinal controlling effect of the region.

Based on the above concept, the time series average value of the summer rainfall amount based on the observed data was found to be 501.7 mm. Based on this reference, model *cccma* was found to be perfect relatively. Whereas, models such as *ipsl, inmcm, giss*, and *echam* under predicts and model *bccr* over predict the summer rainfall amount. Similarly, SD and cv values indicate that model *cccma* was performing well as compared to others (Table 2).

Moreover, it is clear that the magnitude of the root mean square error (rmse) for the observed and forecasted rainfall trends has been smaller for the model *cccma* than the rmse for the rest of the models. Although, the correlations might not support to conclude that the model *cccma* performance, relatively this model captured similar to the observed value in most of the statistical analysis. Model *bccr* also has similar characteristics next to *cccma* and could be useful to consider those model values for future prediction of summer rainfall over Ethiopia.

The graphic representations of the statistical value of the summer means average rainfall amount has clearly shown that model *cccma* more or less similarly captured to that of the observed values. Models such as*bccr, echam* and *giss* also indicted similar patterns to the observed one. Model *bccr* correlation coefficient explained better relationship, however, over prediction was observed by the remaining statistics results (Fig. 2).

After the statistical analysis, the spatial distribution of summer rainfall was generated using grid analysis and display system (GrADS) computer software program. As indicated in the observation (NNRP), the southwestern and central highlands of Ethiopia received maximum summer rain; whereas, the eastern, western and southeastern periphery of the country has received very little summer rain. In a similar manner, the appropriate model, which captured summer rainfall distribution, is model *cccma* and *bccr*. Although the rainfall pattern has indicated by all the models, the spatial rainfall distribution of summer in Ethiopia for the period between 1971 and 1990 clearly captured by the *cccma* and the *bccr* model (Fig. 3).

**Table 2 Statistical analysis of rainfall (1971–1990)**

| Model | Clim (mm) | SD | Cv (%) | Corr | Rmse | Bias |
|---|---|---|---|---|---|---|
| NNRP[a] | 501.7023 | 40.33089 | 8.038809071 | | | |
| *Bccr* | 592.1023 | 54.06119 | 9.130380004 | 0.21042016 | 112.8483 | 90.4 |
| *Cccma* | 546.9452 | 44.3595 | 8.11041033 | 0.13351548 | 62.14697 | 45.2429 |
| *Echam* | 356.2808 | 53.90224 | 15.12914533 | 0.00429265 | 160.1898 | −145.4215 |
| *Giss* | 416.9231 | 22.73914 | 5.454036967 | −0.07013787 | 97.26162 | −84.7792 |
| *Inmcm* | 282.4245 | 49.81025 | 17.63666042 | −0.14229288 | 229.7001 | −219.2778 |
| *Ipsl* | 182.0708 | 36.48957 | 20.04141795 | −0.08403028 | 324.6071 | −319.6315 |

*Clim* climatology (time series average value of rainfall), *Sd* standard deviation, *cv* coefficient of variation, *corr* correlation

[a] NNRP Observed rainfall recorded mean values from satellite, ground based and observation above the top of the stratosphere (reanalysis)

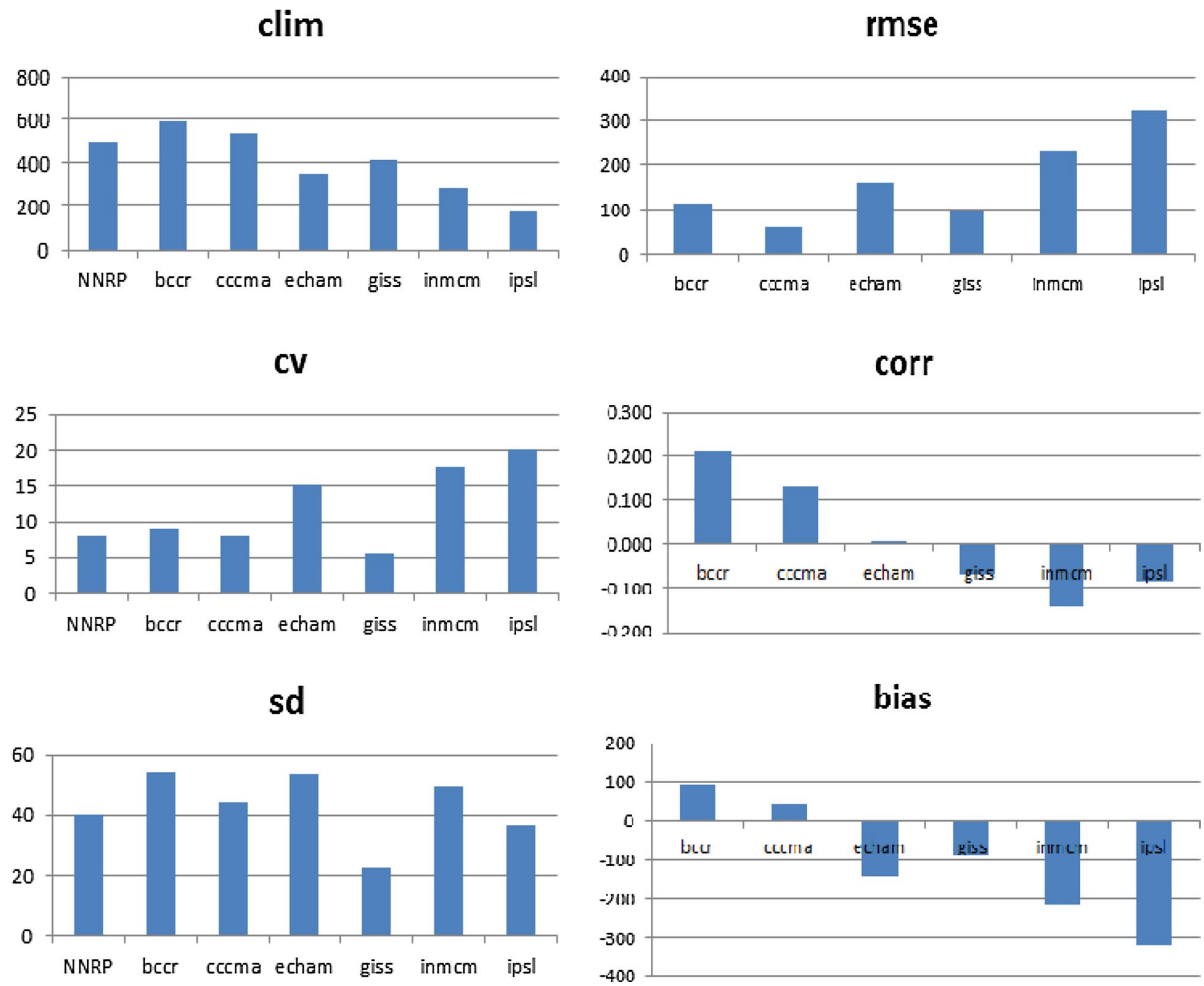


**Fig. 2** The statistical analysis of 1971–1990 rainfall

**Normalized anomaly and probability of detection (POD)**

The normalized anomaly of summer rainfall is the best parameter (probability of observed rainfall transformed into an index). Multiple time scales allow for temporal flexibility in evaluation of rainfall conditions and water supply. It is not merely the "difference of rainfall from the mean divided by the standard deviation", the rainfall data was normalized using a probability distribution so that the values of the index are actually regarded as standard deviations from the median. Normalized distribution allows for estimating both dry and wet periods. Accumulated values can also be utilized to analyze drought severity (magnitude). Probability based (probability of observed precipitation transformed into an index) nature is considerably suited to risk management. Accordingly, values of $-1 < 0<1$ would be taken as normal rainfall amount year, values greater than 1 excess rainfall year and values less than $-1$ would be taken as rainfall deficit year (Doswell et al. 2005). Based on these concepts, the normalized anomaly of the summer rainfall analysis has indicated that the 1972, 1974 and 1982 years showed that deficit; whereas, the 1978 and 1979 were found to be excess rainfall years from the period 1971 to 1990. The rest of the years were found to be normal (Table 3).

The probability of detection was calculated by dividing the frequency of the model matching with the observed value. In other words, the number of hit rate or the number of times in which the model output matches to the observation. Accordingly, the number of years which were in rainfall excess was only 1978 and 1979; whereas, the hit match of model *bccr* was one (1978). Probability of detection (POD) (hit rate) then calculated by dividing the number of hit matches (one) to the number of excess years (two), which was found to be 0.5. This implies that the hit rate of model *bccr* to capture similar value to that of the observed was 50 %. Similarly, the hit rate of the

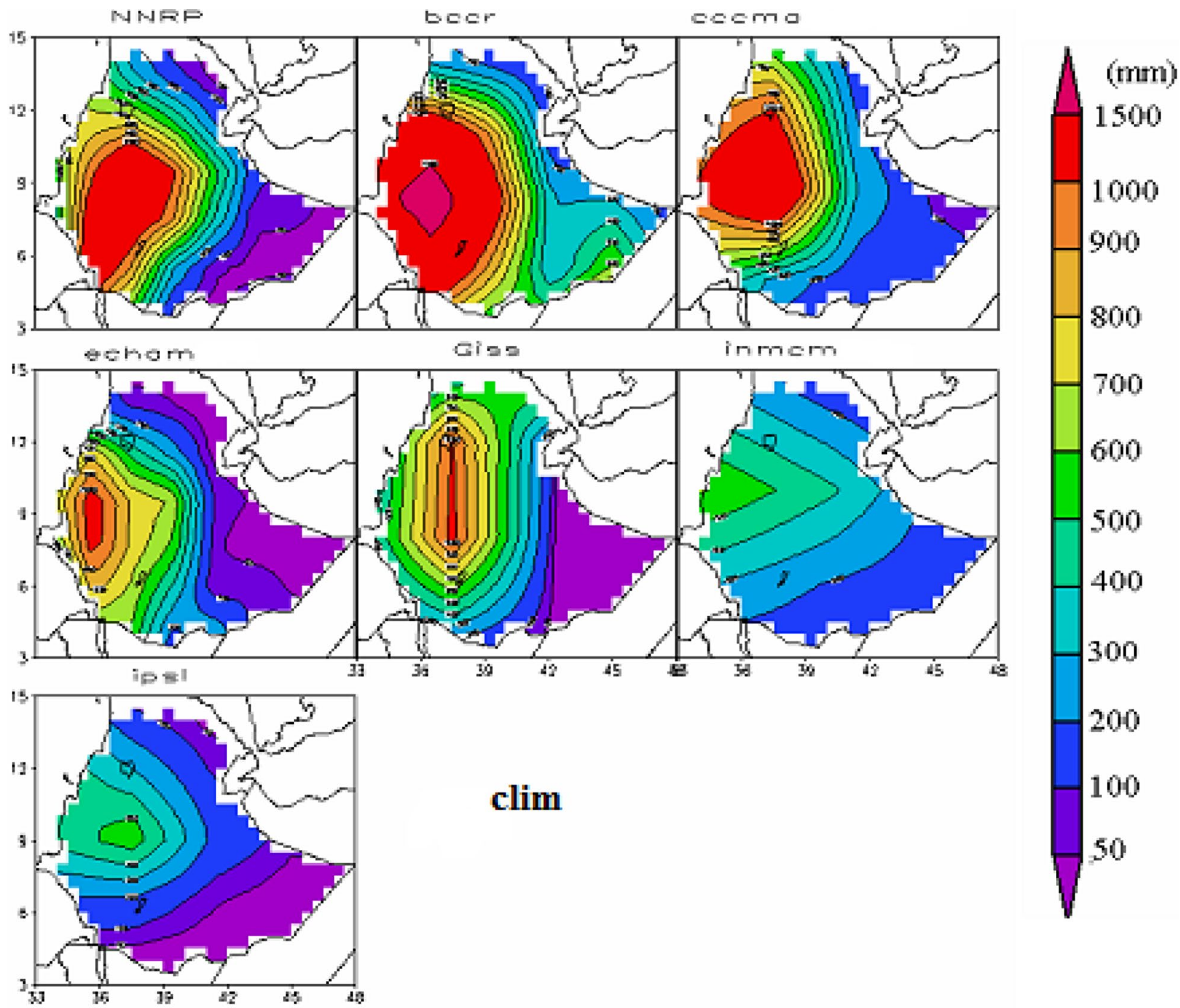


**Fig. 3** Spatial distribution of Ethiopian summer monsoon in GCM and NNRP

model on excess rainfall amount for the model *cccma* and *echam* computed to be 50 %. On the other hand, the hit rate on excess rainfall for the models *giss, inmcm* and *ipsl* found to be 0 %. It implies that the probability of the model to capture similar value to the observed (NNRP) is 0 %. In a nutshell, model *bccr, cccma* and *echam* performed better than *giss, inmcm* and *ipsl* models in capturing excess rainfall of the period 1971–1990. The deficit frequency of the observed years found to be three, (1972, 1974 and 1982); however, none of the models matches those years' records. The POD for all of the models for deficit years of the period 1971–1990 found to be 0 % (Table 4).

The frequency of the normal rainfall years was found to be 15, whereas, the frequency of the models which matches the observed one were (*bccr* = 9, *cccma* = 13, *echam* = 10, *giss* = 12, *inmcm* = 10 and *ipsl* = 11). The hit rate found to be (*bccr* = 0. 6, *cccma* = 0.87, *echam* = 0. 67, *giss* = 0. 8, *inmcm* = 0. 67 and *ipsl* = 0.73). Based on this value, the highest POD value has recorded by model *cccma* (0.87). This value also supports that the performance of the model *cccma* was found to be the best by capturing similar normal rainfall values of the observed one.

The overall performance of the models was measured by the combined matching frequencies. This can be done by dividing the frequency of the total matching (deficit, excess and normal) rainfall to the total model values. For instance the frequency of the total matching rainfall of the model *bccr* was (deficit = 0, excess = 1 and normal = 9). The combined POD was calculated by dividing the sum of the frequency of deficit, excess and normal

**Table 3 Summer rainfall amount normalized anomaly**

| Year\model | *NNRP* | *Bccr* | *Cccma* | *Echam* | *Giss* | *Inmcm* | *Ipsl* |
|---|---|---|---|---|---|---|---|
| 1971 | 0.153 | −1.412 | −0.853 | −0.858 | −0.571 | −1.568 | −0.300 |
| 1972 | −1.881[a] | −0.175 | 0.848 | −0.144 | −0.945 | −0.608 | −0.513 |
| 1973 | −0.819 | −0.037 | 0.562 | 0.669 | 1.045 | −0.385 | 0.150 |
| 1974 | −1.858[a] | 0.400 | 1.145 | −0.204 | 1.027 | 0.768 | 0.359 |
| 1975 | 0.521 | −1.191 | −0.587 | −0.469 | 0.709 | 0.004 | 2.499 |
| 1976 | −0.907 | 1.790 | −0.043 | 1.805 | −2.360 | 0.115 | 0.084 |
| 1977 | 0.813 | 0.702 | 2.684 | −1.053 | −0.908 | 1.279 | 1.609 |
| 1978 | 1.755[b] | 1.399 | −0.806 | −1.002 | −0.195 | −0.909 | −1.348 |
| 1979 | 1.294[b] | −0.572 | 1.041 | 2.319 | −0.648 | −0.875 | −1.173 |
| 1980 | −0.519 | 0.094 | 0.021 | 1.699 | 0.365 | −0.504 | −0.989 |
| 1981 | 0.634 | 0.288 | −0.415 | 0.432 | −0.001 | −1.106 | 0.063 |
| 1982 | −1.493[a] | −0.714 | −0.880 | −0.554 | 0.269 | −0.605 | 0.104 |
| 1983 | −0.456 | 0.799 | −0.432 | −1.529 | −0.582 | −0.194 | 0.572 |
| 1984 | 0.977 | 0.461 | −0.621 | 0.290 | −0.192 | −0.945 | 0.396 |
| 1985 | 0.447 | 1.723 | 0.723 | 0.486 | 0.711 | 0.131 | −1.433 |
| 1986 | 0.880 | −1.083 | 0.876 | −0.029 | −0.275 | −0.435 | 0.284 |
| 1987 | −0.046 | −0.693 | −0.607 | −1.229 | 2.574 | 0.929 | −0.396 |
| 1988 | 0.840 | −1.645 | 0.173 | 0.047 | −0.393 | 0.703 | −0.646 |
| 1989 | −0.149 | 0.836 | −0.948 | −0.299 | 0.981 | 2.206 | 1.574 |
| 1990 | −0.187 | −0.969 | −1.880 | −0.379 | −0.609 | 1.997 | −0.895 |

[a] Deficit

[b] Excess rainfall years

**Table 4 Models probability of detection (POD)**

| Model | Excess | Deficit | Normal | Combined |
|---|---|---|---|---|
| *Bccr* | 0.5 | 0 | 0.60 | 0.50 |
| *Cccma* | 0.5 | 0 | 0.87 | 0.70 |
| *Echam* | 0.5 | 0 | 0.67 | 0.55 |
| *Giss* | 0 | 0 | 0.8 | 0.6 |
| *Inmcm* | 0 | 0 | 0.67 | 0.5 |
| *Ipsl* | 0 | 0 | 0.73 | 0.55 |

rainfall years by the total model years (10/20). Accordingly, the best performed model from the overall analysis of POD calculations was the model *cccma* (70 %) (Tables 4, 8). In general, we have concluded that from the period 1971 to 1990, the model *cccma* captured relatively similar rainfall recorded vales as compared to the observed one.

### Summer monsoon in the GCM and the observed (1991–2010)

The statistical analysis of the observed data revealed that the summer rainfall amount of the period 1990–2010 time series average, standard deviation and coefficient of variation found to be 431.19 mm, 39.14 and 9.0776, respectively (Table 5).

As usual, those models which captured closely related rainfall value to the observed rainfall values would be performed better. Accordingly, model *giss's* clim, SD and cv values were more similar than the rest of the models. The second model that has relatively similar clim value is *echam* (Table 6). However, model *inmcm* has closer sd value than *echam* and model *bccr* has relatively closer cv value than *giss*. It implies that model values in capturing similar statistical rainfall value were not uniform except *giss* model. On the other hand, the model values recorded least by rmse and bias could perform best. Model *giss* then capture relatively the least rainfall value by those statistics mentioned above. The statistical correlation and partial correlation computed, but unable to indicate the best performed model. With irrespective of the poor indication of correlation coefficient values, model *bccr* has relatively higher relationship with the observed value. In general, the model *giss* could be used for better predictions of the future summer rainfall in Ethiopia based on the period 1990–2010.

It is clearly indicated in the Fig. 4 that the model *giss*, *bccr* and *cccma* appears best by recording relatively similar rainfall recorded values of the observed.

GrADS output for the period 1991–2010 confirm that most of the models have captured similar summer rainfall distribution. Unlike the 1971–1990 period where a

**Table 5 Statistical analysis of summer rainfall (1991–2010)**

| Model | Clim (mm) | SD | Cv | Corr | Rmse | Bias |
|---|---|---|---|---|---|---|
| *NNRP* | 431.19 | 39.14 | 9.08 | | | |
| *Bccr* | 529.09 | 67.84 | 12.82 | 0.31 | 93.51 | 97.90 |
| *Cccma* | 522.56 | 69.29 | 13.26 | −0.04 | 89.75 | 91.37 |
| *Echam* | 353.61 | 59.56 | 16.84 | −0.29 | 111.59 | −77.58 |
| *Giss* | 421.44 | 35.13 | 8.34 | 0.00 | 53.51 | −9.75 |
| *Inmcm* | 290.64 | 36.25 | 12.47 | 0.13 | 149.11 | −140.55 |
| *Ipsl* | 179.77 | 25.89 | 14.40 | −0.29 | 256.89 | −251.42 |

**Table 6 Summer rainfall amount normalized anomaly (1991–2010)**

| Year\model | *NNRP* | *Bccr* | *Cccma* | *Echam* | *Giss* | *Inmcm* | *Ipsl* |
|---|---|---|---|---|---|---|---|
| 1991 | −0.580 | 0.763 | 1.218 | −0.035 | 0.040 | 2.227 | −1.015 |
| 1992 | 0.485 | −0.667 | 0.095 | 1.815 | −1.616 | 1.048 | −0.326 |
| 1993 | −1.149[a] | −0.588 | 0.000 | 0.295 | −0.171 | −0.225 | 0.950 |
| 1994 | 0.397 | 0.279 | 1.557 | −0.652 | −0.849 | 0.623 | −1.301 |
| 1995 | −1.002[a] | −1.344 | −0.179 | 1.900 | 0.432 | −1.851 | 1.200 |
| 1996 | 0.285 | 1.162 | 1.624 | 0.909 | −1.708 | 0.379 | 0.962 |
| 1997 | −0.497 | 1.899 | −0.811 | −0.959 | 0.519 | 1.426 | 1.773 |
| 1998 | −0.034 | −1.192 | 1.553 | −0.370 | −1.439 | 0.626 | −0.060 |
| 1999 | −0.194 | −0.386 | 0.100 | 0.517 | 0.009 | 0.763 | −0.763 |
| 2000 | −1.064[a] | 0.721 | −0.068 | −1.034 | 0.201 | −0.462 | −0.090 |
| 2001 | 0.274 | −0.525 | −1.847 | 0.385 | 1.442 | −0.152 | 1.530 |
| 2002 | −1.136[a] | 0.647 | −0.098 | −1.019 | −0.289 | −1.093 | 0.351 |
| 2003 | −0.132 | 0.283 | −0.405 | −1.489 | 0.136 | −0.388 | −0.903 |
| 2004 | −1.153[a] | 1.631 | −0.398 | 0.286 | −0.852 | −1.460 | −0.893 |
| 2005 | 0.142 | −0.197 | −0.288 | −0.161 | 2.014 | −0.364 | 1.565 |
| 2006 | −0.052 | 1.125 | −1.085 | 1.516 | −0.084 | 0.042 | −0.542 |
| 2007 | 1.358[b] | −0.691 | −2.166 | −0.427 | −0.401 | −1.473 | −1.678 |
| 2008 | −1.008[a] | −1.601 | 0.612 | 0.725 | 1.476 | −0.187 | 0.214 |
| 2009 | 1.847[b] | 0.064 | 0.082 | −1.556 | 1.343 | 0.869 | −0.551 |
| 2010 | 2.714[b] | −1.383 | 0.501 | −1.044 | −0.203 | −0.346 | −0.423 |

[a] Deficit

[b] Excess rainfall years

single model was highly performed by capturing summer rainfall distributions, the summer rainfall distribution of the period 1991–2010 has captured by more than one model. As it has depicted by Fig. 5, model *bccr, cccma, echam* and *giss* capture more or less similar summer rainfall pattern to that of the observed one. This created an alternative for further predictions of Ethiopian summer than ever before.

The summer rainfall normalized anomaly values of the observed data which indicated deficit were the year 1993, 1995, 2000, 2004 and 2008; whereas, the excess rainfall years were recorded in 2007, 2009 and 2010. The remaining years were normal rainfall (Table 6). The hit rate of each model was then counted and resulted in the deficit years by model *bccr* and *echam* two times and by model *inmcm* three times. On the other hand, model *cccma*, *giss* and *ipsl* didn't capture deficit rainfall years. Similarly, the hit rate of the models for excess rainfall years were not captured by models *bccr, cccma, echam, inmcm* and *ipsl*. They have captured, but couldn't match to the observed value. In the case of normal rainfall years model *echam* captured the highest number of hit rate (eight times), *bccr* the second highest (seven times) and model *ipsl* and *giss* captured six times each. This implies that the normal years have been captured better than the deficit and excess years by most of the models.

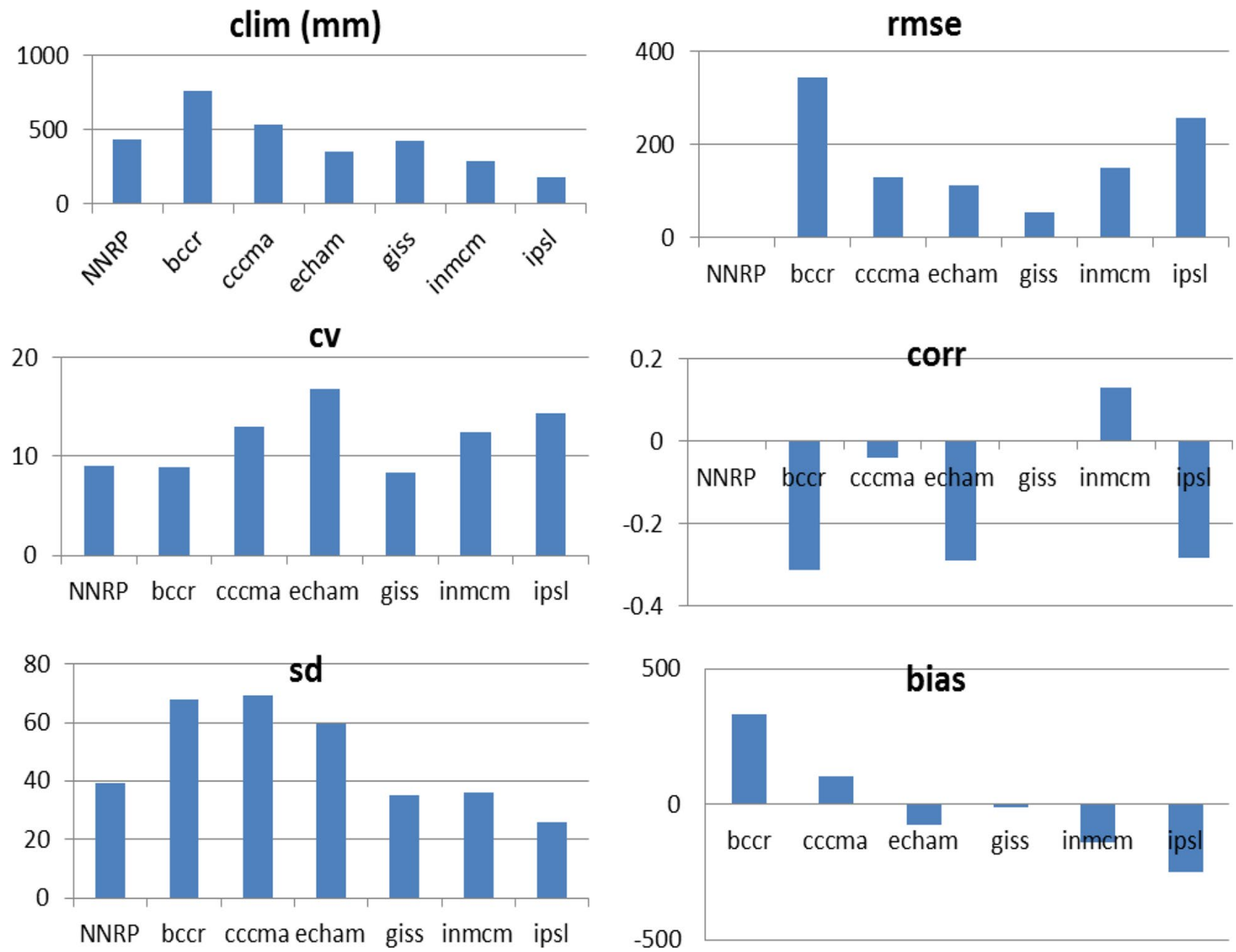


**Fig. 4** Graphic representations of the statistical analysis of 1991–2010 rainfall

The POD for all the models to capture excess rainfall has been found to be 0 % except *igss* which is 33 %. On the other hand the POD for deficit rainfall years has been better by the model *inmcm* (50 %), *bccr* and *echam* (33.3 %) and *giss* (16.7 %). However, model *cccma* and *ipsl* were not captured deficit rainfall years (0 % POD). The POD percentage of the model *inmcm* and *echam* were 72.73 %. These models captured relatively better than the others did (bccr = 63.64 %, cccma = 45.46 % and *ipsl* and *giss* = 54.55 %).

The overall model performance were then calculated from the total frequency of matching to the total years and model *echam* and *inmcm* (55 %) were shown best performance (Table 7).

In the final analysis, from the period 1990 to 2010, it has been found that model *giss* appears best based on the statistical value; whereas, model *echam* and *inmcm* appears to be best based on POD. It implies that most of the models captured more or less similar results to that of the observed and can be used for future predictions.

**Summer monsoon outlooks (2015–2034)**

Predicting the future outlooks of Ethiopian summer rainfall has been done based on the best-performed model results by capturing Ethiopian climate in the above section. For better comparisons and considerations, the analysis has done for all models which performed better and which did not. Most of the models failed to capture Ethiopian summer rainfall due to the fact that the altitudinal climate controlling effects have been dominating than the latitudinal one. Accordingly, the future summer rainfall amount of Ethiopia was done by dividing into two periods (2015–2034 and 2035–2054).

The prediction of the rainfall by the period 2015–2034 was based on the statistical analysis of the model, which performed best in the historical summer monsoon.

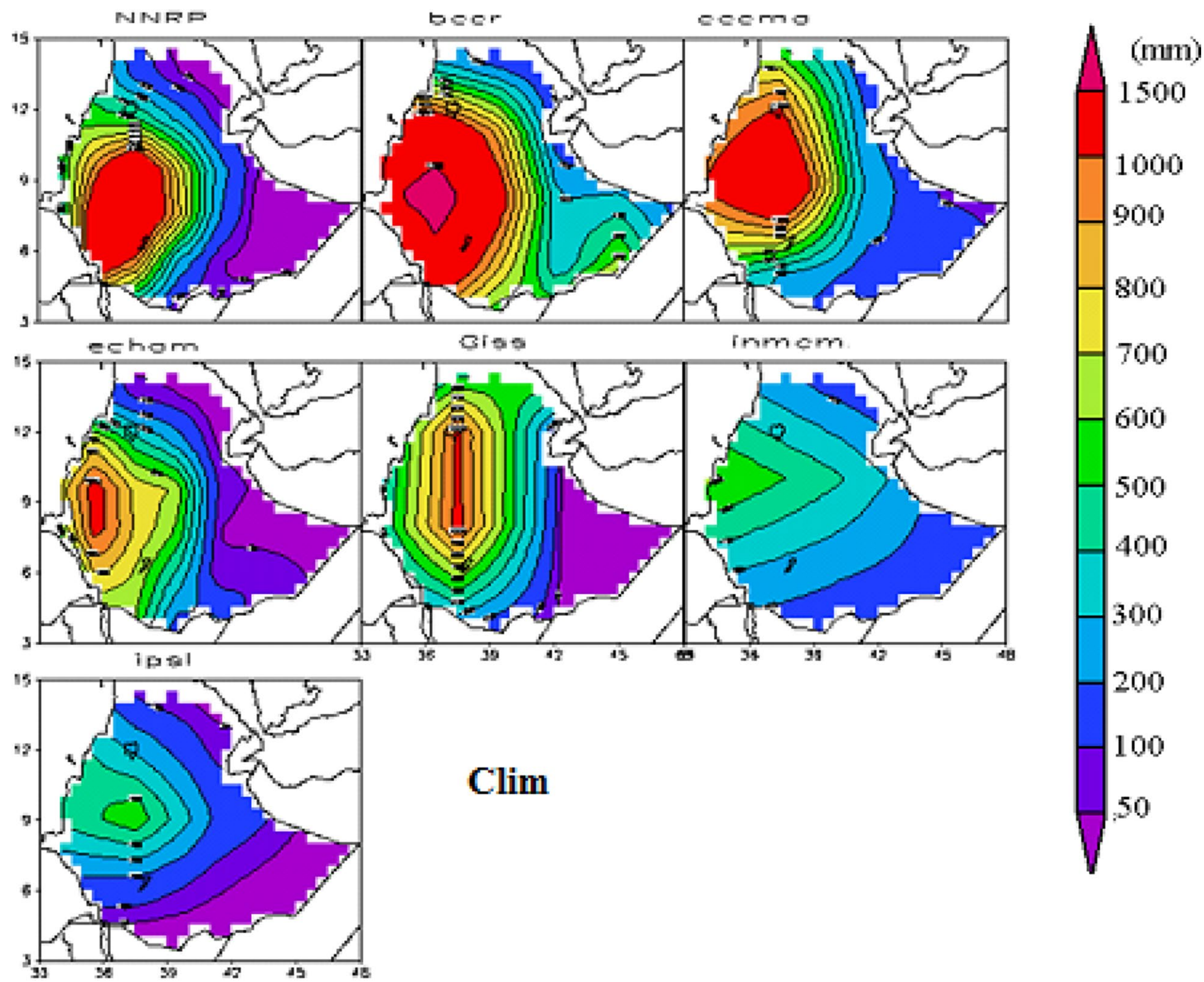


**Fig. 5** Spatial distribution of Ethiopian summer monsoon in GCM and NNRP

**Table 7 Probability of detection (POD) (1991–2010)**

| Model | Excess | Deficit | Normal | Combined |
|---|---|---|---|---|
| *Bccr* | 0 | 0.333 | 0.6364 | 0.45 |
| *Cccma* | 0 | 0 | 0.4546 | 0.25 |
| *Echam* | 0 | 0.333 | 0.7273 | 0.55 |
| *Giss* | 0.33 | 0.167 | 0.5455 | 0.40 |
| *Inmcm* | 0 | 0.50 | 0.7273 | 0.55 |
| *Ipsl* | 0 | 0 | 0.5455 | 0.30 |

Accordingly, model *giss*, *cccma*, *echam* and *inmcm* have been captured relatively closer value (412.45, 520.92, 512.62 and 298.27 mm) for clim, respectively. Based on this result, the values of the model *giss* and *echam* were closet; however, the standard deviation of rainfall from *echam* showed that higher deviations from the normal than the standard deviation of *giss*. Similarly, the coefficient of variation of rainfall from *echam* was higher than the coefficient of variation of the rainfall from *giss* model (Table 8). *Giss* model captured more or less constant amount of rainfall for the study period. In a nutshell, *giss* model could be relatively performed best; however, this model has shown a general constant and or a slight increase of rainfall in contrary to the observed value and could not be used to predict the future. However, model *cccma* and *bccr* relatively indicate that a general decline of rainfall which are in line with the observation trends. Based on these models, it has been predicted that summer rainfall of Ethiopia indicated a general decline.

The summer rainfall distribution predictions also supported the above conclusion that model *giss* and *echam* clearly depicted the pattern. However, it was hardly acceptable to use *giss* model values since it has

**Table 8 Statistical analysis of summer rainfall (2015–2034)**

| Model | Clim (mm) | SD | Cv |
|---|---|---|---|
| *Bccr* | 512.6278 | 71.46301 | 13.9405257 |
| *Cccma* | 520.9299 | 38.08747 | 7.31143864 |
| *Echam* | 378.4397 | 64.74207 | 17.1076317 |
| *Giss* | 412.4507 | 34.00297 | 8.24412954 |
| *Inmcm* | 298.2686 | 37.25766 | 12.49131 |
| *Ipsl* | 183.0517 | 25.81825 | 14.10435 |

insignificant trend changes in the historical data analysis. It has indicated that constant amount of rainfall which was not recorded by the observed data. However, model *bccr* and *cccma* have shown that a similar pattern to the observed data with a slight over predictions was recorded. This was confirmed by the patterns of the summer rainfall amount (Fig. 6).

The normalized anomaly table has shown that all of the models recorded deficit, excess and normal years. The frequency of recording deficit rainfall years were four except model *echam* (three); whereas, the frequency of excess rainfall predicted years by all the models were three. According to model *bccr*, the year 2020, 2023, 2027 and 2033 have been found to be rainfall deficit; whereas, the year 2015, 2022 and 2026 predicted to be excess rainfall. The remaining years have been predicted to be normal rainfall occurrence. On the other hand, the years, which were confirmed by more than one model on the rainfall to be a deficit, normal and excess, can support the probability of its occurrence. For instance, the year 2015 and 2020 were predicted by excess summer rain by two models (*bccr* and *echam*). And years such as 2016, 2017, 2023 and 2029 were predicted by two models as summer rainfall deficit (Table 9). Prediction of a year by more than one model increases the probability of occurrence of the extreme as well as the normal rainfall distributions. These indications will play a significant role for the rural summer rain-fed agricultural dependent people. Governmental and non-governmental bodies also consider these predictions in their plans and programs while designing sustainable development in the region. Hence, precautionary measures will minimize the adverse impacts of those climate related hazards once the perfect predictions were stated.

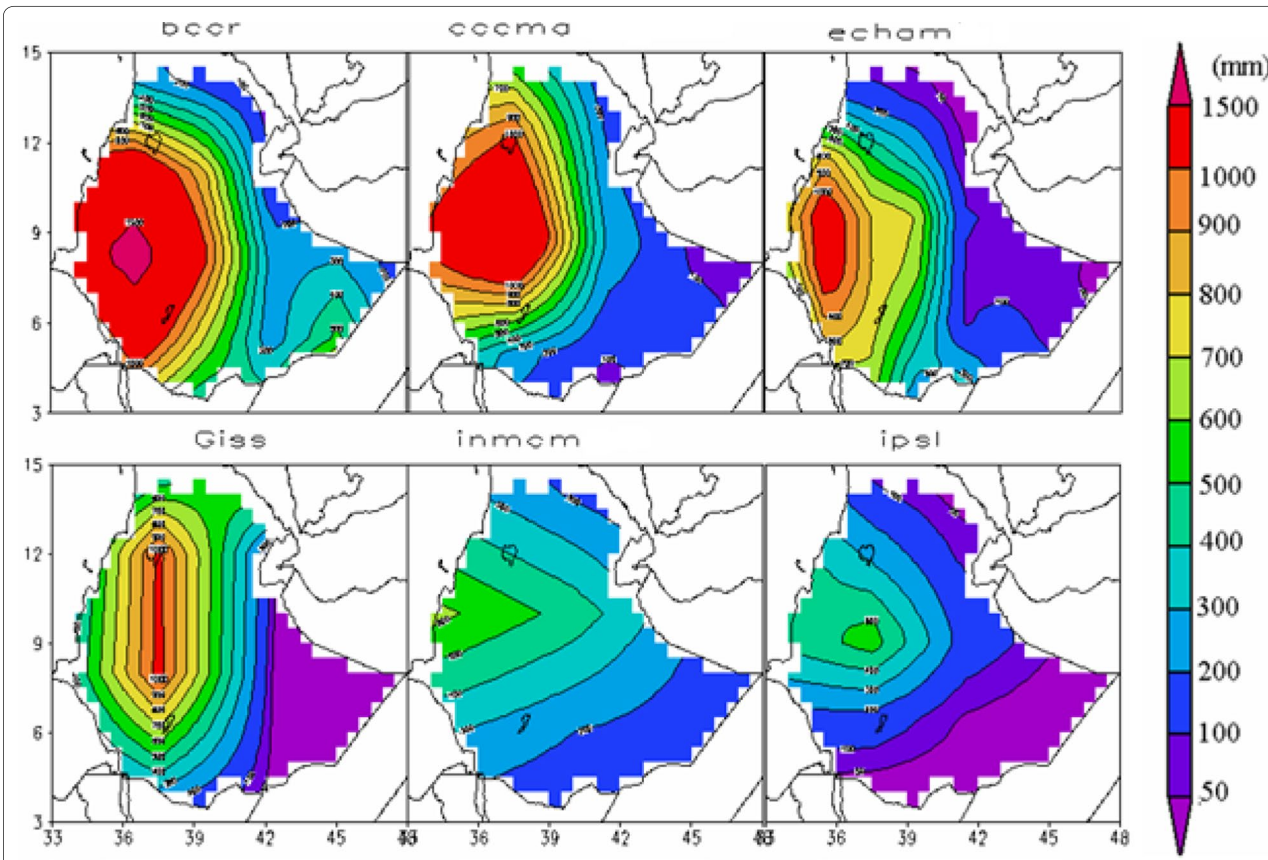


**Fig. 6** Spatial distribution of Ethiopian summer monsoon (2015–2034)

**Table 9 Summer rainfall amount normalized anomaly (2015–2034)**

| Year\model | *Bccr* | *Cccma* | *Echam* | *Giss* | *Inmcm* | *Ipsl* |
|---|---|---|---|---|---|---|
| 2015 | 1.268 | 0.025 | 1.014 | −0.092 | 0.946 | 0.144 |
| 2016 | −0.653 | 0.339 | 0.465 | −1.566 | 0.140 | −2.280 |
| 2017 | 0.138 | −2.502 | −1.686 | −0.958 | 0.463 | 1.489 |
| 2018 | −0.868 | −0.770 | 0.200 | −1.286 | −0.272 | −0.943 |
| 2019 | 0.837 | 0.973 | 1.495 | 0.173 | −0.057 | 0.626 |
| 2020 | −1.447 | 0.196 | 0.918 | 0.176 | 1.080 | 2.014 |
| 2021 | 0.689 | 0.036 | −1.287 | 1.712 | −0.625 | −0.137 |
| 2022 | 1.594 | −0.390 | 0.728 | 0.552 | −0.106 | −1.027 |
| 2023 | −1.044 | −1.770 | 1.593 | −0.389 | −0.463 | −0.202 |
| 2024 | −0.861 | 0.584 | −0.542 | 1.210 | −1.482 | 0.941 |
| 2025 | 0.678 | 1.411 | −0.417 | 0.319 | 0.911 | −1.107 |
| 2026 | 1.975 | 0.919 | 0.921 | 0.683 | 2.061 | −0.176 |
| 2027 | −1.012 | −0.116 | 0.353 | 1.207 | 0.390 | −0.861 |
| 2028 | 0.105 | −1.112 | −0.899 | 0.986 | 0.432 | −0.119 |
| 2029 | 0.225 | −0.225 | 0.290 | −1.716 | −1.864 | 0.438 |
| 2030 | 0.977 | −1.037 | −0.588 | −0.326 | −0.908 | 0.494 |
| 2031 | −0.103 | 1.256 | −0.784 | −1.610 | 0.305 | 0.286 |
| 2032 | −0.634 | 0.832 | 0.755 | 0.953 | −1.064 | 1.153 |
| 2033 | −1.739 | −0.153 | −0.783 | −0.446 | 1.260 | −1.058 |
| 2034 | −0.326 | 1.203 | −1.844 | 0.316 | −1.448 | 0.224 |

**Summer monsoon outlooks (2035–2054)**

By this sub period, the model value of clim by *giss* and *echam* were found to be 422.13 and 400.36 mm, respectively. However, the value of the standard deviation for *echam* (95.51) deviated more than *giss* (47.44). Similarly the coefficient of variation of *echam* (23.86) is much greater than that of *giss* (11.24). Though those models seemed to record similar rainfall amount, unable to use them for accurate predictions due to the low hit rate of models. Instead, model *bccr* and *cccma* values were used to predict the summer monsoon outlooks (Table 10). The historical analysis of those models helps to easily decide this case about the accurate prediction of the future rainfall conditions. By taking into consider the value of model *bccr* and *cccma*, the decision makers can take precautionary measures to minimize the risk of the hazards created as a result of extreme rainfall occurrence.

**Table 10 Statistical analysis of summer rainfall (2035–2054)**

| Model | Clim | SD | Cv |
|---|---|---|---|
| *Bccr* | 423.1752 | 125.5509 | 29.6687755 |
| *Cccma* | 460.8515 | 62.06466 | 13.4673881 |
| *Echam* | 350.3633 | 95.51073 | 27.2604836 |
| *Giss* | 422.1384 | 47.43772 | 11.2374804 |
| *Inmcm* | 302.4444 | 55.19686 | 18.2502503 |
| *Ipsl* | 171.6467 | 33.69273 | 19.6291161 |

The graphic representations of the rainfall analysis have shown in the Fig. 7. Based on this, the three models (*bccr, cccma* and *echam*) recorded more or less similar record for both periods (2015–2034 and 2035–2054). These models also show good performance in recording a closer rainfall value to the observed one in the historical analysis. Therefore, it should be taken into consider the future rainfall status in planning for sustainable livelihoods of the rural people of Ethiopia.

The GrADS output of the predicted summer rainfall distribution better represented by the model *bccr* and *cccma* (Fig. 8). Based on the patterns of rainfall, the first four models have recorded in a similar trends; whereas, the last two models have failed to capture the Ethiopian rainfall pattern. From the above analysis and its historical similarity to the observed rainfall records, model *bccr* has been appeared to predict the future fate of Ethiopian summer rainfall.

The 2035–2054 rainfall normalized anomaly table has shown that more number of years has been found to be a deficit as compared to the period 2015–2034. Model *echam, giss* and *inmcm* predicted six, seven and six rainfall deficit years, respectively; whereas, model *bccr and ipsl* four and model *cccma* five deficit years have been predicted. This implies that the frequency of rainfall deficit years has increased across models. On the other hand, the years 2035, 2037, 2045, 2046 and 2047 have been confirmed by more than two models as rainfall deficit

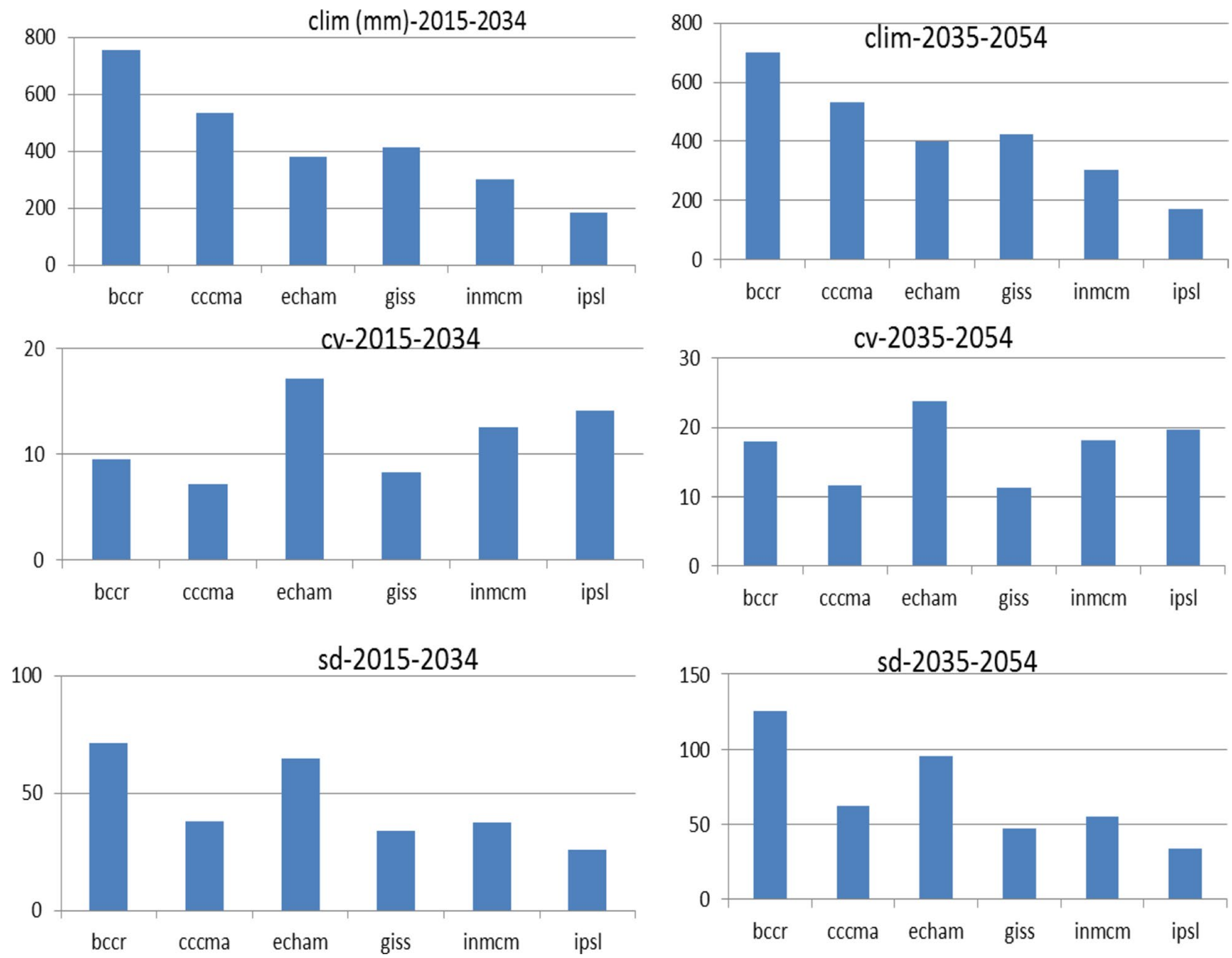


**Fig. 7** Graphic representations of the statistical rainfall analysis

years, which increased the probability of the occurrence of deficit, which might lead to drought (Table 11). However, it should be noted that the prediction values of the best performed model in the historical analysis would be more trusted predictions than the rest of the models. Hence, this indication would give an insight to the concerned body for the proper planning and implementation of strategies.

Model output data analysis supported the ground based station data. More than one year were recorded in the rainfall deficit years in the last full point between the years (2035 and 2054) than the first period (1971–1990). Rainfall is certainly the most significant element influencing the success or failure of rural livelihoods (agricultural production). It demonstrates itself through its effect on soil, plant growth, as well as on every phase of animal development and growth. Crop and animal disease are the direct consequence of any fluctuations of rainfall in the study area. Nevertheless, crop losses can be scaled down substantially by affecting adjustments through timely and through accurate predictions and prognoses. This backup also provides guidelines for long range or seasonal planning and choice of crops best suits to the anticipated rainfall conditions.

## Conclusions

By analyzing the GCM data output and the National Center for Environmental Predictions (NCEP) re-analysis of the period 1971–2010, the trend analysis and the future predictions (2015–2054) have been stated by a comparative method. According to the observed meteorological data, the past Ethiopian summer monsoon has declined by 70.51 mm Table 12.

Most of the models have failed to capture Ethiopian summer rainfall due to the fact that the altitudinal climate controlling effects have been dominating than the latitudinal one. The heterogeneous topography of the country as well as the mountainous domination of its

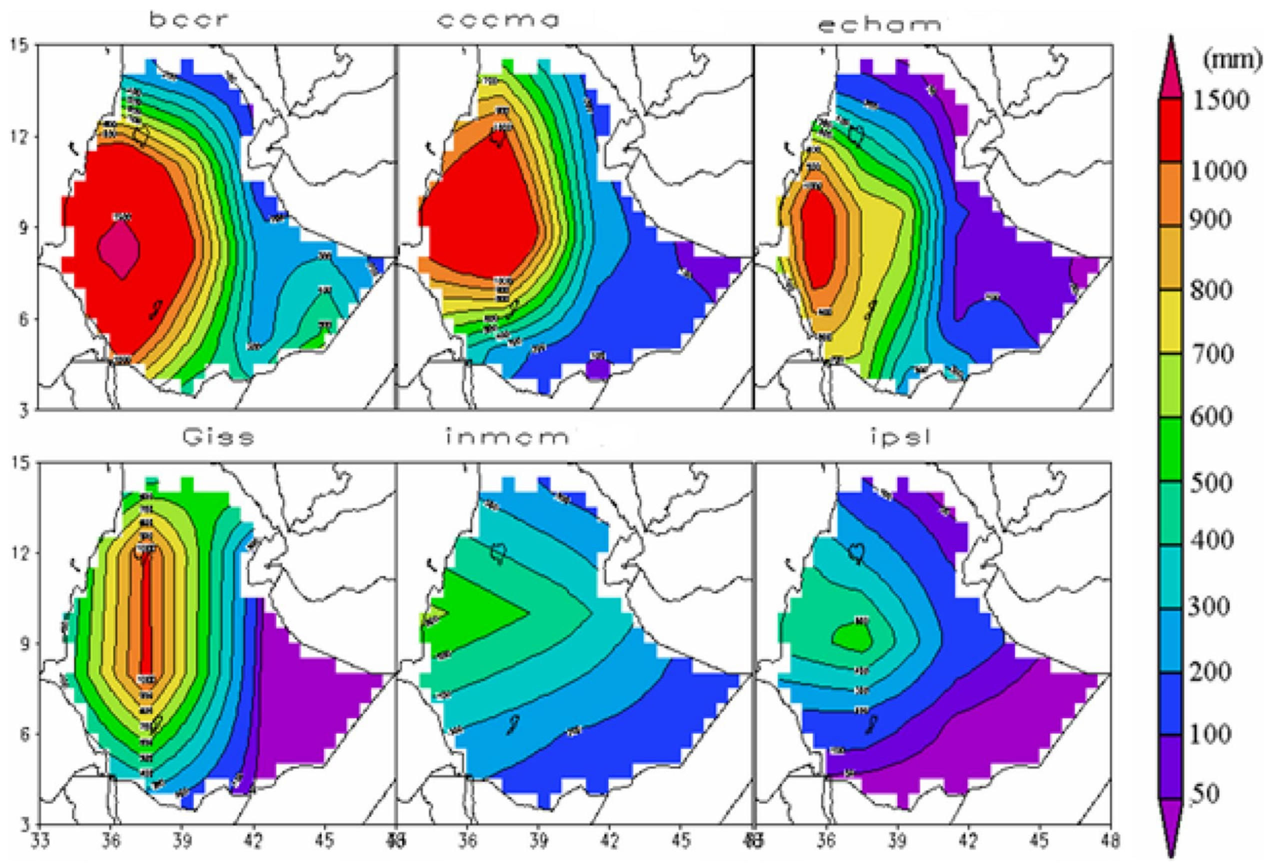


**Fig. 8** Spatial distribution of Ethiopian summer monsoon in GCM (2035–2054)

**Table 11 Summer rainfall amount normalized anomaly (2035–2054)**

| Year\model | *Bccr* | *Cccma* | *Echam* | *Giss* | *Inmcm* | *Ipsl* |
|---|---|---|---|---|---|---|
| 2035 | 1.203 | 0.739 | *−1.605* | *−1.003* | −0.503 | *−1.713* |
| 2036 | −0.297 | *−1.064* | 1.614 | *−1.024* | −0.423 | 1.335 |
| 2037 | −0.006 | *−1.240* | *−1.050* | 0.051 | −0.964 | *−1.052* |
| 2038 | 0.162 | 0.569 | *−1.027* | *−1.027* | 0.152 | 0.192 |
| 2039 | 0.554 | −0.315 | 2.238 | 1.426 | −0.098 | −0.306 |
| 2040 | *−1.000* | −0.745 | 0.985 | *−1.165* | 1.478 | −0.187 |
| 2041 | 0.049 | 0.403 | −0.331 | −0.411 | *−1.167* | −0.390 |
| 2042 | *−1.362* | 0.996 | −0.314 | 0.960 | 0.651 | *−1.014* |
| 2043 | 0.877 | −0.632 | 0.196 | 0.151 | −0.950 | 0.139 |
| 2044 | 0.147 | *−1.142* | 0.255 | 1.442 | *−1.287* | 1.429 |
| 2045 | *−1.764* | −0.134 | 0.800 | *−1.099* | *−1.167* | 1.559 |
| 2046 | *−2.020* | 1.725 | *−1.043* | *−1.982* | −0.367 | 1.260 |
| 2047 | −0.215 | 0.238 | *−1.642* | *−1.829* | *−1.233* | −0.190 |
| 2048 | 0.148 | 1.683 | 1.305 | −0.577 | −0.997 | −0.781 |
| 2049 | −0.342 | 1.315 | 0.461 | −0.133 | 0.019 | −0.322 |
| 2050 | 0.812 | *−1.013* | *−1.047* | −0.045 | 0.627 | 0.068 |
| 2051 | 0.222 | 1.082 | −0.279 | 0.254 | *−1.005* | −0.471 |
| 2052 | 1.227 | −0.522 | −0.542 | 1.481 | 1.774 | −0.536 |
| 2053 | 2.158 | *−1.719* | −0.445 | 1.316 | 1.605 | 2.047 |
| 2054 | −0.653 | −0.325 | 0.072 | −0.651 | *−1.159* | *−1.366* |

**Table 12 Summary of monsoon analysis (1971–1990 and 2015–2054)**

| Period | *NNRP* | *Bccr* | *Ccma* | *Echam* | *Giss* | *Inmcm* | *Ipsl* |
|---|---|---|---|---|---|---|---|
| 1971–1990 | 501.7023 | 592.1023 | 546.9452 | 356.2808 | 416.9231 | 282.4245 | 182.0708 |
| 1991–2010 | 431.1891 | 529.0888 | 522.562 | 353.6072 | 421.4417 | 290.6424 | 179.7729 |
| Difference | −70.5132 | −63.0135 | −24.3832 | −2.6736 | 4.5186 | 8.2179 | −2.2979 |
| 2015–2034 | | 512.6278 | 520.9299 | 378.4397 | 412.4507 | 298.2686 | 183.0517 |
| 2035–2054 | | 423.1752 | 460.8515 | 350.3633 | 422.1384 | 302.4444 | 171.6467 |
| Difference | | *−89.4526* | *−60.0784* | *−28.0764* | 9.6877 | 4.1758 | −11.405 |

landscapes, Ethiopia dominantly experienced a temperate type climatic zone though located within the tropics. The heterogeneous characteristics of the landscape enabled the task of climate modeling difficult. By the comparative analysis of the models' data outputs, the best performed models having similar trends to the observed data predicted the future summer monsoon as a decline of 89.45 mm by model *beccr* to 60.07 mm by model *cccma*. To conclude, the legislative bodies and development planners should design strategies and plans by taking into account impacts of declining summer rainfall on rural livelihoods.

**Acknowledgements**
This study would never be completed without the contribution of many people to whom I would like to express my gratitude. Professor P.V.V.Prasada Rao, Murali Negasa Rao, and Meteorology and Oceanography staff of the Andhra University, and finaly to the Bahir Dar University, College of Agriculture and Environmental Sciences staff for their academic contribution during data collection, analysis and write up of this research.

**Competing interests**
The author declare that he has no competing interests.

Received: 14 February 2016 Accepted: 25 March 2016
Published online: 14 April 2016

**References**

Compo GP, Whitaker PD, Sardeshmukh N, Matsui RJ, Allan X, Yin BE, Gleason RS, Vose G, Rutledge P, Bessemoulin S, Brönnimann M, Brunet RI, Crouthamel AN, Grant PY, Groisman PD, Jones M, Kruk AC, Kruger GJ, Marshall M (2011) The Twentieth Century Reanalysis Project. Q J Roy Meteorol Soc 137:1–28. doi:10.1002/qj.776

CSA(Central Statistical Agency) (2007) Central Statistical Agency Population and Housing Census of Ethiopia, Addis Ababa. Retrieved August 2013 from CSA database

Doswell CA, Harold EB, Michael PK (2005) Climatological estimates of daily local non-tornadic severe thunderstorm probability for the United States, vol 20. American Meteorological Society, Boston, p 577

Gulilat TD, Thomas T, Len S (2008) Ethiopian rainfall in climate models. Retrieved April 2013 from http://climate.ncas.ac.uk/len/african_climate/ethiopia_climate_models_draft_nofigs.pdf

IPCC (2007) Synthesis report contribution of working group i, ii and iii to the fourth assessment report of the intergovernmental panel on climate change core writing team. In: Pachauri RK, Reisinger A (eds). IPCC, Geneva, p 104

IPCC-DDC (2007) Model output archive run by program for climate model diagnosis and inter-comparison (PCMDI). Retrieved May 2013 fromhttp://www.ipcc-data.org/gcm/monthly/SRES_AR4/index.html'

Joel BS, Mike H (2006) Climate change scenario handbook climate research unit. University of East Anglia, Norwich, p 35

Maugeri HY (2011) The twentieth century reanalysis project. Q J Roy Meteorol Soc 137:1–28. doi:10.1002/qj.776

McSweeney C, New M, Lizcano G (2008) UNDP climate change country profile Ethiopia. School of geography and environment. University of Oxford and Tyndall Center for climate change research, Norwich

Mikko H, Jussi N, Alina P, Pasi R (2009) Climate risk management in finishing development cooperation. Ethiopia adapting to climate change, climate screening assessment. Final report, Gaia

NMSA (National Meteorological Service Agency) (2007) Climate Change National Adaptation Program of Action (NAPA) of Ethiopia. NMSA, Addis Ababa. Retrieved June 23 2013 from NMSA database

Yatagai A, Osamu A, Kenji K, Haraku K, Masato I, Atsushi H (2009) A 44 year daily gridded precipitation data set for Asia based on a dense network of rain gauges SOLA (5), 137–140. doi: 10.2151/sola.2009-035

**Submit your manuscript to a SpringerOpen journal and benefit from:**

- ► Convenient online submission
- ► Rigorous peer review
- ► Immediate publication on acceptance
- ► Open access: articles freely available online
- ► High visibility within the field
- ► Retaining the copyright to your article

**Submit your next manuscript at ► springeropen.com**